RSC Advances

PAPER

View Article Online
View Journal | View Issue

Cite this: *RSC Adv.*, 2022, **12**, 26297

A strategy to prepare internally-plasticized poly(vinyl chloride) by grafting castor oil onto the PVC chain with three different isocyanates as intermediate bridges†

Tianxiang Deng, Shouhai Li, Xiaohua Yang, Lina Xu, Haiyang Ding and Mei Li *

In this work, three types of internally-plasticized poly(vinyl chloride) materials (PVC-H-C, PVC-TH-C, PVC-IP-C) were prepared by grafting castor oil onto the PVC chain with three different isocyanates as intermediate bridges, respectively. The three different isocyanates were hexamethylene diisocyanate (HDI), trimer of HDI (THDI), and isophorone diisocyanate (IPDI). This method does not need any castor oil pretreatment. The effects of different isocyanates on the plasticizing ability of the internally-plasticized PVC and the thermal stability of the whole material were discussed. The grafting of castor oil onto PVC with hexamethylene diisocyanate (HDI) as the intermediate bridge has the best plasticizing effect among the three types of internally-plasticized poly(vinyl chloride) materials, as the elongation at break reaches 294%, and the glass transition temperature is lower than that of pure PVC from 75 to 58 °C. It is worth mentioning that the thermal stability is optimized when HDI trimer (THDI) is used as the intermediate bridge, which may be related to the triazine ring contained in THDI. Moreover, this PVC material (PVC-TH-C) also has higher decomposition activation energy when the mass loss is 40% and releases less HCl and benzene gas during thermal degradation. The three types of internally-plasticized PVC all show excellent migration resistance, and almost do not migrate in the petroleum ether environment.

Received 20th June 2022
Accepted 8th September 2022

DOI: 10.1039/d2ra03787d

rsc.li/rsc-advances

1. Introduction

Poly(vinyl chloride) (PVC) is the second widely-used polymer globally, and plays a significant role in the global plastic market owing to its low cost.[1] Pure PVC has two disadvantages: easy brittle fracture and poor thermal stability.[2,3] In terms of mechanical properties, PVC is prone to brittle fracture, so it needs to be mixed with a large amount of plasticizers to improve its processability in industrial production.[4] The addition of plasticizer increases the toughness of PVC, making PVC softer and more flexible. Traditional plasticizers such as dioctyl phthalate (DOP) and dibutyl phthalate (DBP)[5,6] have excellent plasticizing effect on PVC. However, these plasticizers easily migrate from the PVC substrate, and are toxic, which will negatively impact the environment and human health.[7] Though some nontoxic plasticizers are prepared (*e.g.* bio-based alkyl terminal hyperbranched polyglycerols,[8] epoxidized castor oil polyol ester,[9] phosphaphenanthrene groups containing soybean oil polyol ester[10]), the preparation methods are still limited by the problem of plasticizer migration, which will also lead to serious decline in the physical properties of PVC products. Therefore, it is very important to inhibit the migration and precipitation of plasticizers. The most effective way to prevent precipitation is to covalently connect plasticizers to PVC. The C–Cl bond of PVC has low energy and can be easily replaced by some nucleophiles, which provides an opportunity for the covalent connection of plasticizers to PVC chain.[11] To comply with the concept of green chemistry, researchers have covalently connected some natural oils and fats to the PVC chain as plasticizers, which can also improve the utilization of natural oils and fats. For internal plasticization of PVC, some methods can be used to graft castor oil methyl ester,[12] phosphorous ricinoleic acid derivatives,[13] epoxidized acetylation castor oil methyl ester and epoxidized soybean oil,[14] aminated tung oil methyl ester[15] and oleic[16] onto PVC chains. The process starts with natural oil, but the natural oil needs pretreatment (*e.g.* methyl esterification or epoxidation), which is complex and increases production costs. Hence, a method that can graft natural oil directly onto PVC can maximize the utilization of raw materials and avoid the cost of natural oil pretreatment.

The low thermal stability of PVC is another major problem of PVC. The normal PVC structure is formed by head-to-tail

Institute of Chemical Industry of Forest Products, CAF; National Engineering Research Center for Low-Carbon Emission & High-Efficiency Processing and Utilization of Forest Biomass;Key Lab. of Biomass Energy and Material, Nanjing, Jiangsu 210042, PR China. E-mail: 1194763279@qq.com; lishouhai1979@163.com; yxh20087@163.com; xulina072@163.com; dinghaiyang2008@163.com; lm@icifp.com

† Electronic supplementary information (ESI) available. See https://doi.org/10.1039/d2ra03787d

copolymerization between molecules of vinyl chloride, but head-to-head or tail-to-tail abnormal structures are easily formed in actual production, which make the C–Cl energy lower than that in the normal structure and subject C–Cl to breakdown. As a result, HCl is easily removed from PVC upon heating, which will cause the failure of the PVC substrate.[17] Furthermore, the extracted HCl will negatively impact human health and the surrounding environment, and nucleophilic substitution reaction will replace some Cl atoms on the PVC chain, so less HCl will be produced when heated. At the same time, the graft on PVC critically impacts the thermal stability of the whole PVC.

In this study, castor oil was grafted onto PVC to realize the internal plasticization of PVC, and this method does not need any pretreatment of castor oil. Moreover, the effects of different isocyanates on the thermal stability of PVC were compared. We found that hexamethylene diisocyanate (HDI) used as the intermediate bridge to graft castor oil onto PVC had the best plasticizing effect and the highest elongation at break. The trimer of HDI (THDI) used as the intermediate bridge had the highest thermal stability and released less harmful gases such as HCl and benzene when heated, reducing the impact on the environment and human health.

2. Experimental

2.1. Materials

All reagents were used as received. PVC was supplied from rhawn.cn (K value 59–55). Potassium carbonate (K_2CO_3) (AR) and tetrahydrofuran (THF) (AR) were obtained from Sinopharm Chemical Reagent Co., Ltd (China). Diethanolamine (DEA) (AR), hexamethylene diisocyanate (HDI) (>99%), hexamethylene diisocyanate trimer (THDI) (>99%), isophorone diisocyanate (IPDI) (>99%), castor oil (AR), dibutyltin dilaurate (AR) and petroleum ether were offered by Shanghai Macklin Biochemical Co., Ltd (China).

2.2. Synthesis of internally-plasticized poly(vinyl chloride) materials

Three types of internally-plasticized poly(vinyl chloride) materials(PVC-H-C, PVC-TH-C, PVC-IP-C) were prepared by grafting castor oil onto the PVC chain with three different isocyanates as intermediate bridges, respectively. Three different isocyanates were hexamethylene diisocyanate (HDI), trimer of HDI (THDI), isophorone diisocyanate (IPDI). The three different isocyanates were grafted onto the PVC chain with diethanolamine as intermediate bridges, respectively, which were subsequently turned into internally-plasticized poly(vinyl chloride) materials(PVC-H-C, PVC-TH-C, PVC-IP-C) by reacting with castor oil. The synthetic routes of PVC-H-C, PVC-TH-C, and PVC-IP-C were illustrated in Fig. 1. In addition, it is possible to occur PVC cross-linking reactions. There may appear small amounts of crosslinked PVCs, which were shown in Fig. S1 (ESI).†

2.2.1. Synthesis of PVC-DEA. PVC (20 g), 16.8 g (0.15 mol) of DEA and 11.04 g (3.61 mol) of K_2CO_3 were dissolved in 200 ml of THF under stirring at 60 °C for 4 h under N_2. Then the reaction system precipitated in petroleum ether, washed several times with petroleum ether and dried in a vacuum oven to form PVC-DEA.

2.2.2. Synthesis of PVC-H, PVC-TH, PVC-IP. Three samples of PVC-DEA (3 g) were each dissolved in 50 ml of THF. Then 6 g (0.036 mol) of HDI, 3 g (0.006 mol) of THDI and 6 g (0.027 mol) of IPDI were added into the three mixtures separately and added a few drops of dibutyltin dilaurate, followed by stirring at 60 °C for 2 h. The resulting mixtures were precipitated with petroleum ether, washed several times with petroleum ether, and vacuum-dried to form PVC-H, PVC-TH and PVC-IP, respectively.

2.2.3. Synthesis of PVC-H-C, PVC-TH-C, PVC-IP-C. PVC-H (3 g), 3 g PVC-TH and 3 g PVC-IP were each dissolved in 50 ml of THF, and added first with 6 g of castor oil and then a few drops of dibutyltin dilaurate. Then the mixtures were stirred at 60 for 2 h and precipitated with petroleum ether. After washing several times with petroleum ether, the mixtures were vacuum-dried to form PVC-H-C, PVC-TH-C and PVC-IP-C respectively.

2.3. Preparation of PVC-H-C, PVC-TH-C, PVC-IP-C, PVC/DOP and PVC films

PVC-H-C (3 g), 3 g of PVC-TH-C and 3 g of PVC-IP-C were dissolved in 50 ml of THF separately. The mixtures were fully and mechanically agitated at 200 rpm and room temperature for 1 h. The products were cast into Petri dishes and dried at 60 °C for 2 days to eliminate traces of the remaining solvent, forming thin films.

PVC (3 g) and 1.2 g of DOP were dissolved in 50 ml of THF under complete mechanical agitation at 200 rpm and ambient temperature for 1 h. The products were cast into Petri dishes and dried at 60 °C for 2 days to discard traces of the residual solvent to form thin films.

PVC (3 g) was dissolved in 50 ml of THF under sufficient mechanical agitation at 200 rpm and room temperature for 1 h. The resulting samples were cast into Petri dishes and dried at 60 °C for 2 days to get rid of traces of the residual solvent to obtain thin films.

2.4. Characterization

The FTIR spectrometer (Nicolet iS50-Thermo Fisher Scientific, USA) was operated within 4000–500 cm^{-1} at a resolution of 4 cm^{-1}.

The ^1H NMR spectrometer (ARX300, Bruker, Faellanden, Switzerland) was run with $CDCl_3$ as a deuterated solvent.

Molecular weights of PVC-H-C, PVC-TH-C and PVC-IP-C were detected on an efficient gel chromatograph (Waters, USA) at 30 °C and flowrate of 1 ml min^{-1} (column: mixed PL gel 300 × 718 mm^2, 25 mm) with THF as the solvent.

Migration stability of each plasticizer was measured at 25 °C according to ASTMD1239-98. PVC-H-C, PVC-TH-C, PVC-IP-C and DOP/PVC films were soaked in petroleum ether as the extraction medium. After 12, 24 or 48 h, the extracted PVC-H-C, PVC-TH-C, PVC-IP-C and DOP/PVC were dried and reweighed. The degree of migration was computed as follows:

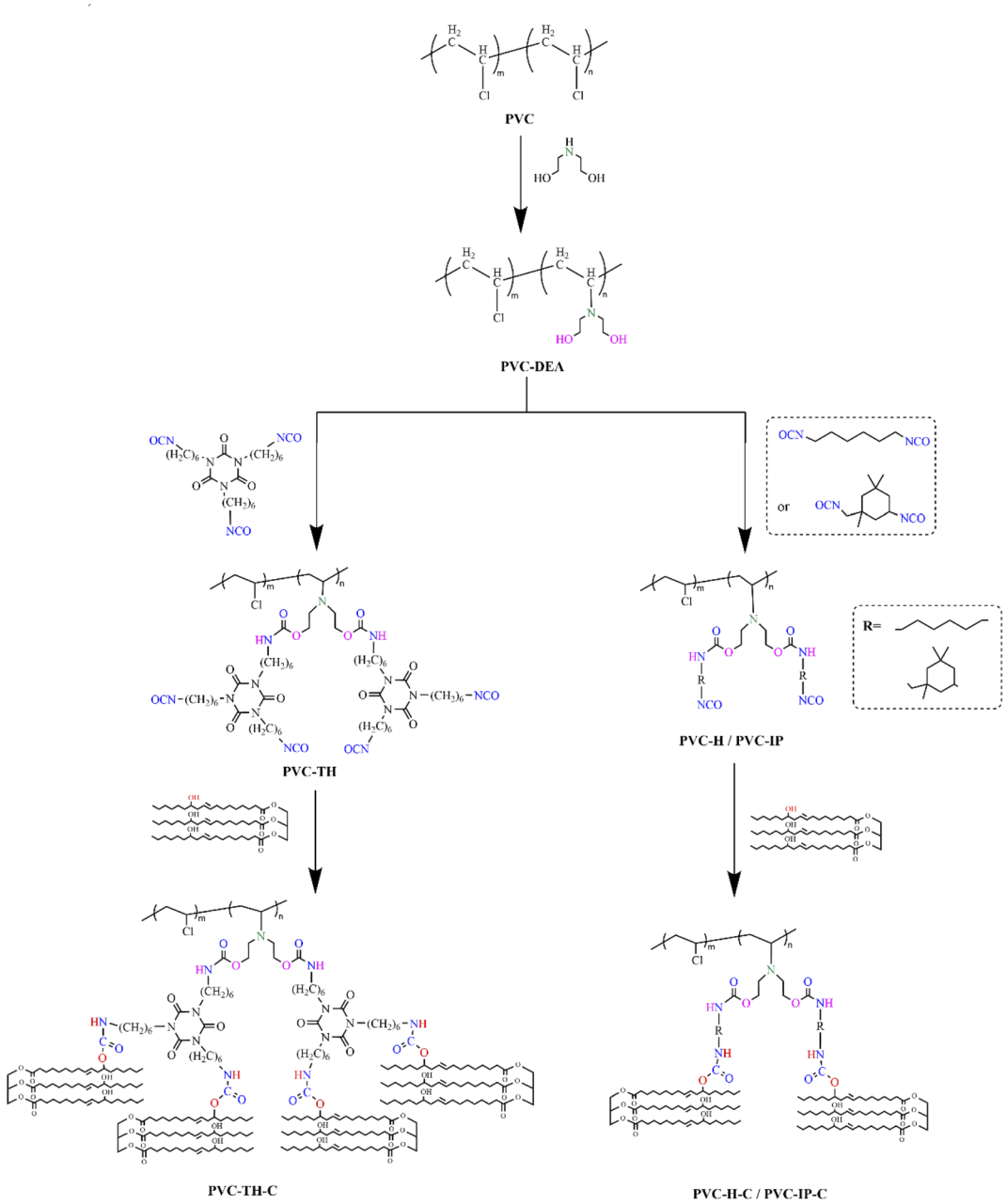

The above synthetic route exclude the generation of cross-linking structure of PVC-TH-C, PVC-H-C and PVC-IP-C. Possible crosslinking structure of PVC-H-C, PVC-TH-C and PVC-IP-C were shown as Fig.S1 in the supplementary material.

Fig. 1 Synthetic route of PVC-H-C, PVC-TH-C and PVC-IP-C.

$$\text{Degree of migration} = \frac{W_1 - W_2}{W_1} \times 100$$

where W_1 and W_2 are the primary and final weights respectively of the tested PVC-H-C, PVC-TH-C, PVC-IP-C or DOP/PVC.

The TA Instruments Q800 dynamic mechanical analyzer (DMA) was run in the tension mode at static force of 0.01 N, oscillatory amplitude of 15 mm, and frequency of 1 Hz. The sample is 15 mm long, 5 mm wide and 1 mm thick.

Tensile strength and elongation at break of PVC, PVC-H-C, PVC-TH-C and PVC-IP-C were recorded as per GB/T 1040-2006 (China) on an E43.104 universal testing device (MTS Instrument Crop., China). The tensile condition is that the force is 50 N and the tensile speed is 20 mm min^{-1}.

The thermal decomposition kinetics of PVC was tested by a Q600 TGA device at the heating rate of 5, 10, 15, 20 or 25 °C min^{-1} and the N_2 flow rate of 100 ml min^{-1} within 30–400 °C.

The 3D gas-phase TGA-FTIR spectra during PVC heated decomposition were recorded on a 409 PC thermal analyzer (Netzsch, Germany) equipped with a Nicolet iS10 FT-IR device.

TG-MS was accomplished with the 409 PC thermal analyzer coupled with a QMS403C device (Netzsch). About 10 mg of a specimen was put into the thermal analyzer under N_2 and heated from 40 to 600 °C at 10 °C min^{-1}.

Discoloration test was conducted according to ISO 305 : 1990 (E). PVC strip films were first put into a XH-314B thermal aging oven (XIHUA, China). The samples were taken out at a certain interval (one sample each time) and their color changes at adjacent time points were observed.

3. Results and discussion

3.1. Structures and characterization of PVC-H-C, PVC-TH-C, PVC-IP-C

The synthesis of the three internally-plasticized PVCs was verified by FT-IR and ^{1}H NMR. The successful grafting of DEA on PVC can be proved by Fig. 2(a and a_1). Compared to the ^{1}H NMR spectra of pure PVC and PVC-H, the peaks at around 4.2 ppm belong to the protons on primary hydroxyl group appeared in the spectrum of PVC-DEA, and the peaks of protons on primary hydroxyl group disappeared in the spectrum of PVC-H. This proves that DEA successfully grafts on the PVC main chain and then reacts with isocyanate. The structures marked in ^{1}H NMR are unique to castor oil. For example, in the castor oil chain segment, the peak of methyl ($-CH_3$) at 0.9 ppm presenting the unique group at the end,[18] and the hydrogen on the carbon connected by the secondary hydroxyl group and the hydrogen on the double bond at 3.7 and 5.4–5.6 ppm prove the introduction of castor oil into the system (Fig. 2(b)). In the spectrum of PVC-HDI, PVC-THDI and PVC-IPDI (Fig. 2(c–e)), because the selected isocyanates are binary or ternary, some isocyanate groups (~2260 cm^{-1}) will be retained after reaction with hydroxyl groups. Meanwhile, the appearance of tertiary amine (3351 cm^{-1}) and disappearance of isocyanate peak in the spectrum of PVC-H-C, PVC-TH-C and PVC-IP-C indicate the successful reaction between isocyanate and hydroxyl, that means the added castor oil completely consumes isocyanate groups. And the reaction between castor oil and PVC-HDI, PVC-THDI and PVC-IPDI is successful. Moreover, the connection of castor oil also increases the molecular weight of the whole material (Fig. S2 in ESI†). Therefore, together with the FT-IR and ^{1}H NMR data, it verifies the successful synthesis of PVC-H-C, PVC-TH-C and PVC-IP-C.

3.2. Mechanical properties of PVC-H-C, PVC-TH-C, PVC-IP-C

Generally, the glass transition temperature (T_g) of a polymer is related to the free volume of molecular chains. In the PVC plasticization with DOP, the mutual movement of PVC chain segments can be simplified due to the large free volume of DOP molecules. Microscopically, these DOP molecules are dispersed between PVC chain segments, and rotate or vibrate to expand the distance between the segments. When the segments mutually move, the mutual interference is small, which leads to low T_g and high flexibility of the material macroscopically. However, pure PVC has a short distance between chain segments and a compact arrangement. When subjected to external force, the interaction between chain segments is large, which makes the pure PVC macroscopically characteristic of brittleness and hardness. Fig. 3(b) shows the T_g values of PVC, PVC-H-C, PVC-TH-C and PVC-IP-C were 75 °C, 58 °C, 92 °C and 71 °C, respectively.

In our work, the internal plasticization mode was studied, and castor oil was grafted on PVC segments. Fig. 3(c) shows three internal plasticizing mechanisms of grafting castor oil onto PVC chain segments. The difference lies in the wide chain agents selected. In the first case (PVC-H-C), because HDI has a linear structure, the connected castor oil segments can vibrate significantly relative to the grafted PVC chain, showing a large

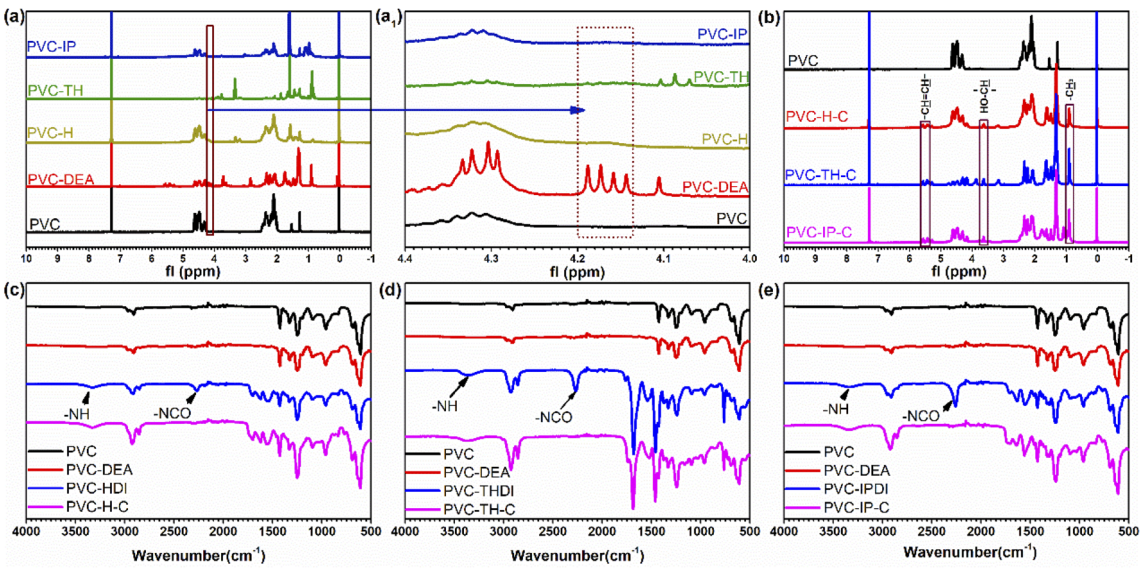

Fig. 2 (a) ^{1}H NMR spectra of PVC, PVC-EDA, PVC-H, PVC-TH and PVC-IP; (a_1) Local ^{1}H NMR spectra of (a); (b) ^{1}H NMR spectra of PVC, PVC-H-C, PVC-TH-C and PVC-IP-C; (c) FTIR spectra of PVC, PVC-EDA, PVC-H and PVC-H-C; (d) FTIR spectra of PVC, PVC-EDA, PVC-TH and PVC-TH-C; (e) FTIR spectra of PVC, PVC-EDA, PVC-IP and PVC-IP-C.

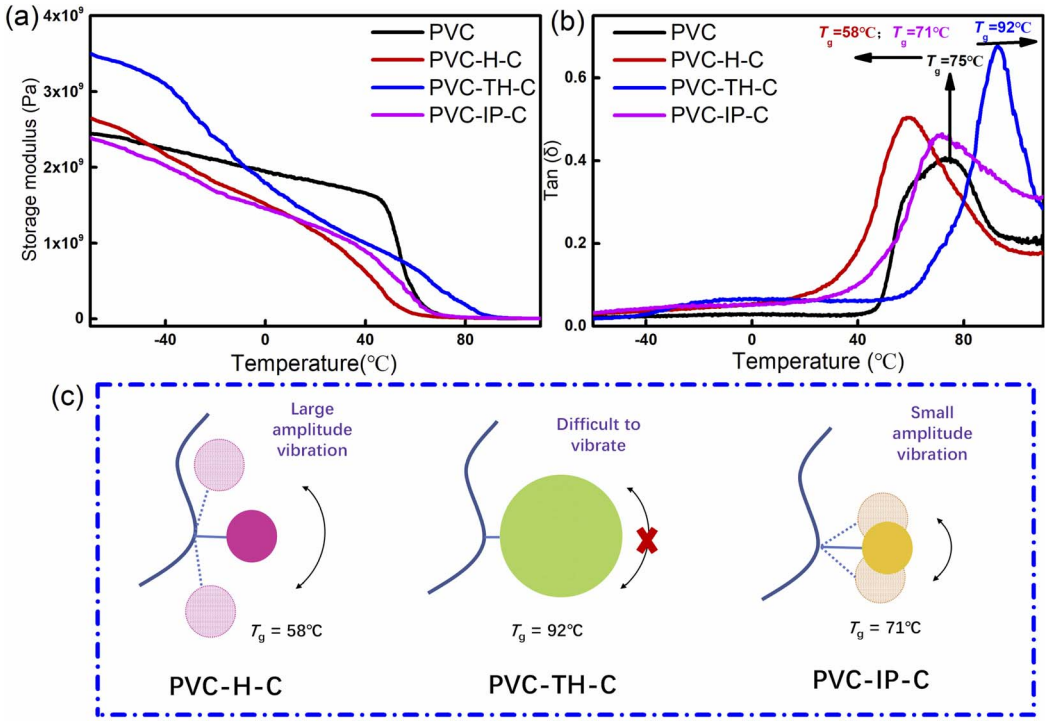

Fig. 3 (a) Storage modulus and tan δ curves of PVC; (b) PVC-H-C, PVC-TH-C and PVC-IP-C. (c) Relationship between T_g and vibration amplitude.

free volume. In the macro-test, the T_g of 58 °C is also lower relative to pure PVC. In the second case (PVC-TH-C), the T_g is 92 °C, which is higher than that of pure PVC. This is because the wide chain agent is the rigid structure of triazine ring, which hinders the vibration of the grafted castor oil chain segments. In addition, because the selected wide chain agent is ternary, ideally, four castor oil molecules can be grafted at the grafting point of one PVC molecule, forming a large steric hindrance. The grafted castor oil is also likely to be self-wound, so the chain segments on the castor oil can also hardly vibrate. The inhibited vibration of the chain segments on the broad chain agent and castor oil leads to a higher T_g than that of PVC. The T_g of PVC-IP-C is in between the first two cases. Because the steric resistance of the six membered ring in IPDI is greater than the linear steric

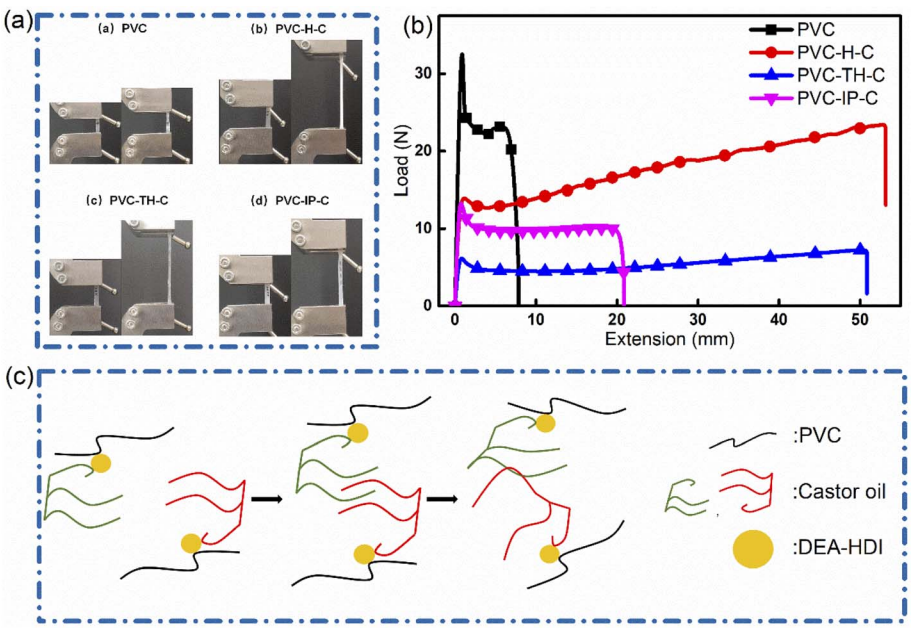

Fig. 4 (a) Stretching diagrams of PVC, PVC-H-C, PVC-TH-C and PVC-IP-C; (b) stretching curves of PVC, PVC-H-C, PVC-TH-C and PVC-IP-C. (c) Schematic diagram of microstretching of PVC-H-C.

Table 1 Tensile strength (T) and elongation at break (E) of PVC, PVC-H-C, PVC-TH-C and PVC-IP-C

Sample	PVC	PVC-H-C	PVC-TH-C	PVC-IP-C
T (MPa)	24.28 ± 2.53	11.23 ± 1.63	12.82 ± 2.36	14.17 ± 2.47
E (%)	40.27 ± 20	280 ± 26	252 ± 5	118 ± 13

resistance in HDI, its vibration amplitude is smaller than that of PVC-H-C, and the resulting free volume is small. Macroscopically, T_g is larger. However, due to the small amplitude vibration, the T_g is still lower than that of pure PVC, which is 71 °C. The storage modulus data show that all storage modulus curves have the same change trend. At - 70 °C, PVC-TH-C has higher storage modulus than those of PVC-H-C and PVC-IP-C (Fig. 3(a)). This is because THDI grafted on PVC-TH-C side chains and castor oil hardly vibrates, and thus can form a relatively orderly and compact stacking structure, which increases the storage modulus at low temperature.

In the tensile tests, the three types of internally-plasticized PVC all show greater elongation at break than pure PVC (Fig. 4(a and b)). Table 1 summarizes the mechanical data of the three kinds of internally plasticized PVC and pure PVC. The highest tensile strength was found in pure PVC (24.28 MPa). Elongation at break values in PVC-H-C, PVC-TH-C and PVC-IP-C increased 444.4%, 375.9% and 114.8%, respectively, over those of pure PVC. Results validates the successful internal plasticization of PVC. The tensile strength representing material rigidity is generally inversely related to the elongation at break representing material flexibility. PVC-H-C shows higher tensile elongation at break than the other two plasticized PVC materials, which can be explained by the network interlocking structure in which winding is severer than crosslinking.[19] Since there are two other branched chains on the grafted castor oil, it is likely to form a winding structure with another PVC. Fig. 4(c) describes this mechanism. This structure can be hardly formed in the other two internal plasticizing modes that hardly vibrate.

Together with the SEM images (Fig. 5), the fracture section of pure PVC is an extremely smooth structure. This is because PVC is a brittle material and is highly sensitive to the impact strength of notches. It shows a typical brittle fracture when damaged at low temperature. At 1.1 k magnification, the fracture sections of the three types of internally-plasticized PVC are relatively and uniformly rough, indicating uniform internally-plasticized PVC materials are prepared by this method. The uneven surfaces of the three types of internally-plasticized PVC materials reflect typical ductile fracture, and the roughness of PVC-H-C is higher, indicating the higher flexibility of PVC-H-C. At higher magnification, the spiderweb-like structure of PVC-H-C can also be found on PVC-TH-C (Fig. S3 in ESII†). The structure on PVC-H-C is the densest, followed by PVC-TH-C, but this structure is not found on PVC-IP-C. These results are also consistent with the tensile test. It is exactly because of this structure that the section becomes coarser and more flexible.

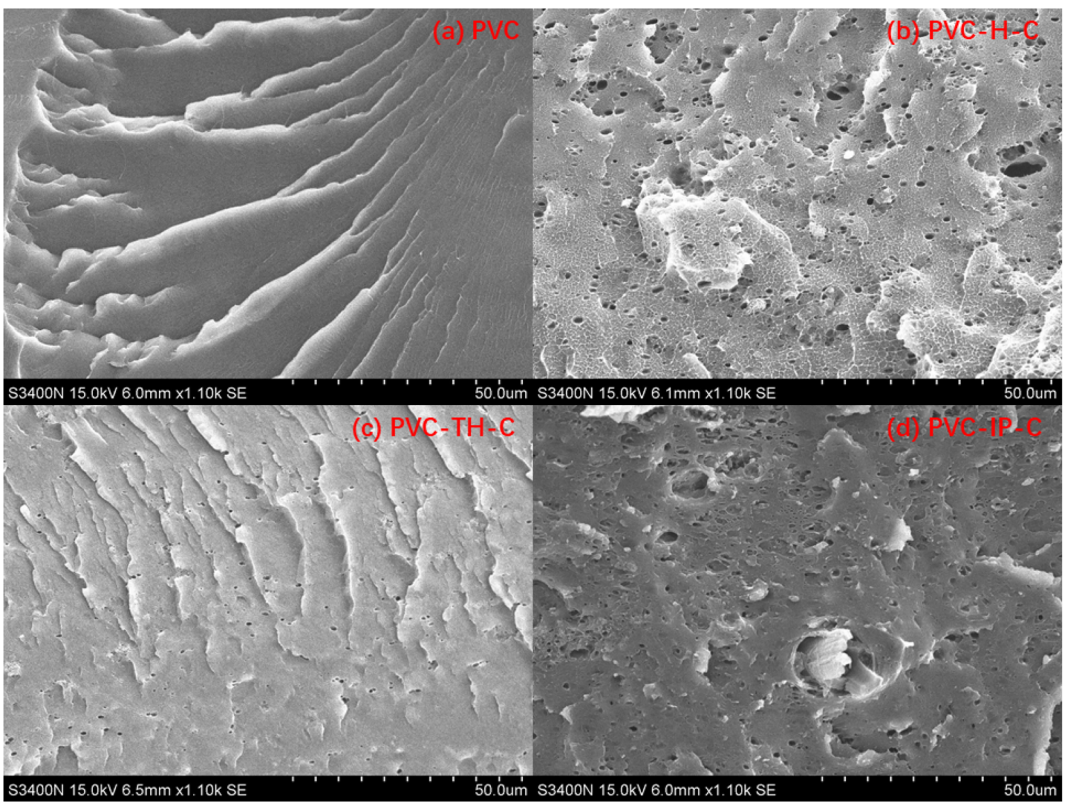

Fig. 5 SEM micrographs of PVC, PVC-H-C, PVC-TH-C and PVC-IP-C.

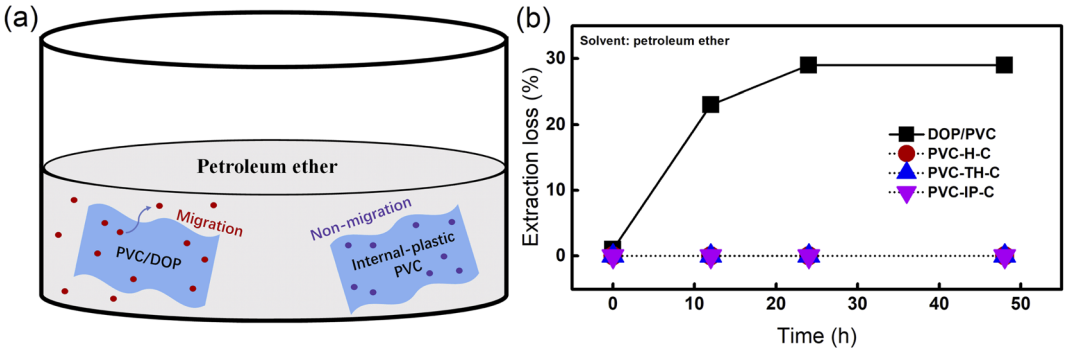

Fig. 6 (a) Migration phenomenon of PVC/DOP and internal-plastic PVC in petroleum ether; (b) degrees of migration of DOP/PVC, PVC-H-C, PVC-TH-C and PVC-IP-C.

3.3. Anti-migration property of PVC-H-C, PVC-TH-C, PVC-IP-C

Under the plasticization condition, the migration resistance of PVC determines the ability of PVC materials to resist environmental risks. Due to the blending mode (physical addition) of traditional plasticizers, plasticizer molecules can be easily "extracted" by the surrounding environment in the PVC chain segments, which not only leads to the failure of mechanical properties of PVC materials but also the great hidden dangers of toxic DOP to the environment and human health. The internal plasticization mode solves this problem well. Because castor oil is covalently connected, rather than physically blended, to the PVC chain, it will not cause migration or precipitation, which ensures the mechanical properties of PVC materials and maintains environmental health. We conducted anti-migration tests after soaking in petroleum ether for 12, 24 and 48 hours. After the test, basically no migration or precipitation of plasticized PVC occurred in the three types of blends, while almost all PVC materials with DOP precipitated (Fig. 6(b)). The inner-plasticized PVC in the experiment may be used in some strongly polar solvents. Fig. 6(a) describes this phenomenon.

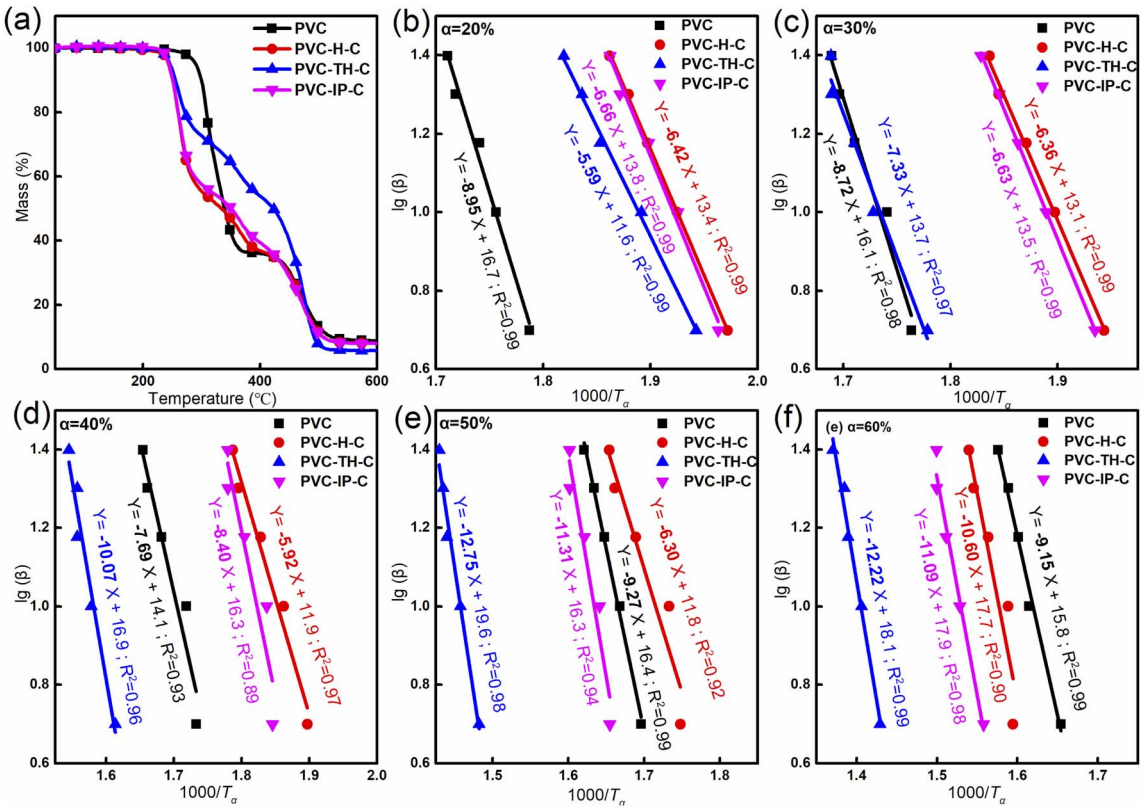

Fig. 7 (a) TGA thermograms of PVC, PVC-H-C, PVC-TH-C and PVC-IP-C. (b–f) Linear plots of log β *vs.* $(1000/T_\alpha)$ based on the Doyle equation (b: $\alpha = 20\%$; c: $\alpha = 30\%$; d: $\alpha = 40\%$; e: $\alpha = 50\%$; f: $\alpha = 60\%$).

Table 2 Decomposition activation energy (E_α (kJ mol^{-1})) of PVC, PVC-H-C, PVC-TH-C and PVC-IP-C under different mass losses

	PVC	PVC-H-C	PVC-TH-C	PVC-IP-C
$\alpha = 20\%$	162.93	116.87	101.76	121.24
$\alpha = 30\%$	158.74	115.78	133.44	120.70
$\alpha = 40\%$	144.90	107.77	183.32	152.92
$\alpha = 50\%$	168.76	114.69	232.11	205.89
$\alpha = 60\%$	166.57	192.97	222.46	201.89

3.4. Thermal properties of PVC-H-C, PVC-TH-C, PVC-IP-C

Thermal stability is another important property of PVC materials. PVC is formed by the polymerization of vinyl chloride head-to-tail in the ideal state, but the abnormal head-to-head or tail-to-tail structure is easily formed in actual processing, which makes the C–Cl energy on these structures significantly lower than that on the normal structure. Due to many defects on the chain segment, the quality loss and color change of PVC after removal of HCl when heated leads to air pollution and failure of optical properties. Under heating conditions, the color of PVC varies from white to yellow, then to brown, and ultimately completely black. Studying the thermal stability of PVC is important and ensures that it does not easily degrade under thermal conditions and maintains high transparency and whiteness (Fig. S4 in ESI†).

Theoretically, we measured the activation energy of PVC materials during degradation using the TGA kinetic method. Fig. 7(a) provides TGA data of PVC and the three internally-plasticized PVC materials. Clearly, the initial decomposition temperature of PVC is higher than those of the three internally-plasticized PVC materials, which three begin to decompose at the same temperature because of the castor oil decomposition on the side chains. PVC-H-C and PVC-IP-C have similar thermal decomposition curves, which means they have similar thermal decomposition processes. The decomposition process of PVC-TH-C (Fig. 7(a)) is obviously difficult, which may be related to the existence of triazine ring in the wide chain agent. The thermal decomposition resistance of triazine ring was already studied previously. Here, to further study the theoretical data of PVC decomposition, we calculated the decomposition activation energy of PVC materials under different mass losses using the TGA kinetic method. Table 2 summarizes the data of total activation energy.

The TGA dynamics research method is calculated based on Doyle equation:[20]

$$\frac{d\alpha}{dT_\alpha} = \frac{A}{\beta} e^{-E_\alpha/RT_\alpha} (1-\alpha)^n \quad (1)$$

$$\frac{d\alpha}{(1-\alpha)^n} = \frac{A}{\beta} e^{-E_\alpha/RT_\alpha} dT_\alpha \quad (2)$$

$$F(\alpha) = \int_0^\alpha \frac{d\alpha}{(1-\alpha)^n} = \int_0^{T_\alpha} \frac{A}{\beta} e^{-E_\alpha/RT_\alpha} dT_\alpha \quad (3)$$

$$\lg \beta = \lg\left[\frac{AE_\alpha}{RF(\alpha)}\right] - 2.315 - 0.4567\frac{E_\alpha}{RT_\alpha} \quad (4)$$

where R is the molar gas constant (8.314 J (mol^{-1} K^{-1})); A is the apparent preexponential factor; T_α is the temperature

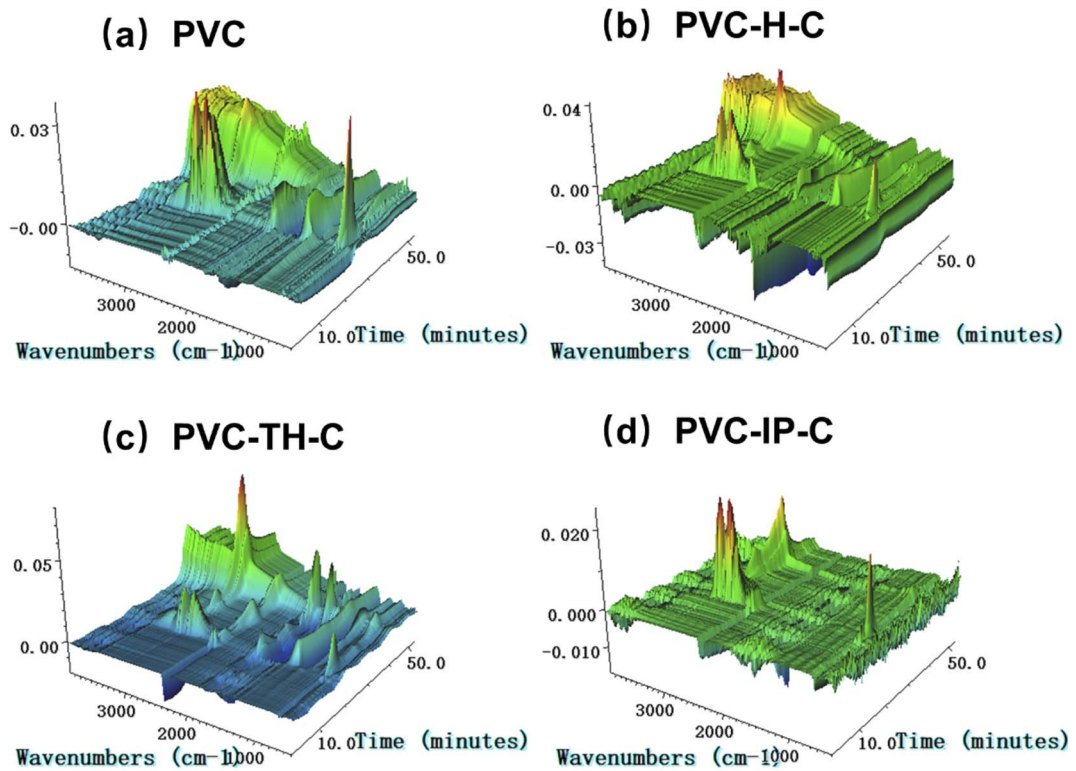

Fig. 8 3D TG-IR spectrum (a–d) of gas from PVC, PVC-H-C, PVC-TH-C and PVC-IP-C.

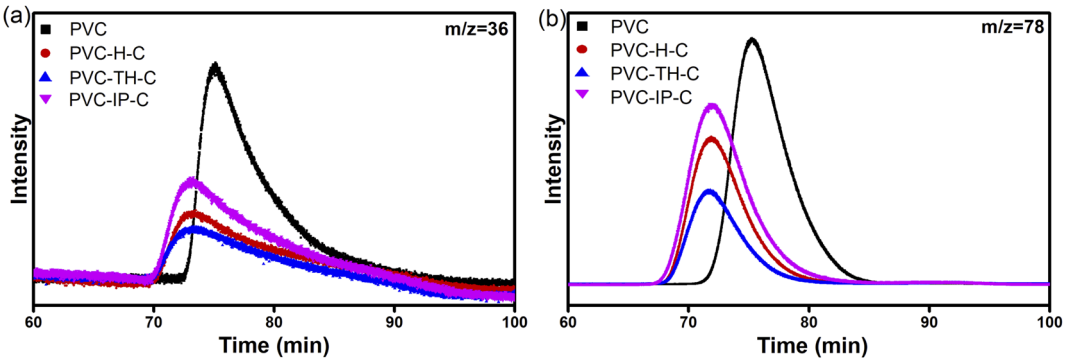

Fig. 9 MS signals (a and b) of main degradation gases from PVC, PVC-H-C, PVC-TH-C and PVC-IP-C.

corresponding to 20%, 30%, 40%, 50% and 60% mass loss in the thermal analysis curve; E_α is apparent activation energy.

Eqn (3) shows that $\log \beta$ and $1/T_\alpha$ are linearly related, and their mapping forms a straight line. E_α is estimated from the slope M of the straight line through eqn (4), and the linear correlation can be determined at the same time:

$$E_\alpha = -M\frac{R}{0.4567} \quad (5)$$

When the mass loss is 0–30%, the decomposition difficulty of pure PVC is higher than that of the three types of internally-plasticized PVC. When the mass loss reaches 40% and above, the decomposition activation energy of PVC containing triazine ring is significantly higher than that of pure PVC and the other two internally-plasticized materials, suggesting that the castor oil internally-plasticized PVC material with THDI as a wide chain agent has less mass loss.

Fig. 8 provides the gas signals generated during the thermal degradation of PVC and three kinds of internal plasticized PVC. The gas signals generated are roughly the same: water: 3500–4000, 1500–1600 cm^{-1}, benzene: 3029 and 1460 cm^{-1}, CO_2: 2372 cm^{-1}, HCl: 2856 cm^{-1}, ester group: 1743, 1267 and 1103 cm^{-1}.[21–23] Castor oil is grafted on the chain segments of the inner-plasticized PVC, which increases the overall carbon equivalent of the material. Compared with the degradation of pure PVC, it will produce more CO_2 in the thermal degradation (Fig. S5 in ESI†). The internally-plasticized PVC nucleophilically substitutes the chlorine atoms on the PVC chain. The Cl level in the system is less than that of pure PVC, so less HCl is produced in the degradation and the environmental harm is reduced (Fig. 9(a)). At the same time, the three types of internally-plasticized PVC also produce less benzene gas than pure PVC during degradation (Fig. 9(b)). After removal of HCl from the pure PVC chain segments, conjugated olefins are produced. These conjugated olefins form aromatic structures such as benzene ring through molecular rearrangement. However, since the three types of internally-plasticized PVC are grafted with castor oil, conjugated olefins that can form aromatic structures such as benzene ring can be hardly formed, further reducing benzene formation. Therefore, compared with pure PVC materials, internally-plasticized PVC materials can release less harmful gases such as HCl and benzene during thermal degradation, reducing damages to the environment and humans. Especially, PVC-TH-C produces less HCl and benzene vapor during thermal degradation, which may be related to the triazine ring in the materials.

4. Conclusions

Castor oil was grafted onto the PVC chain with three wide chain agents (HDI, THDI and IPDI) to plasticize PVC, and thus PVC-H-C, PVC-TH-C and PVC-IP-C were prepared respectively. PVC-H-C had the best plasticity and toughness among the three types of internally-plasticized poly(vinyl chloride) materials, elongation at break values in PVC-H-C, PVC-TH-C and PVC-IP-C increased 444.4%, 375.9% and 114.8%, respectively, over those of pure PVC. The T_g values of PVC, PVC-H-C, PVC-TH-C and PVC-IP-C were 75 °C, 58 °C, 92 °C and 71 °C, respectively. PVC-H-C showed greater tensile strength and elongation at break than PVC-TH-C and PVC-IP-C, which may be related to the intertwining between the linear segments of HDI and castor oil. Compared with PVC/DOP, the three types of internally-plasticized PVC all showed good anti-migration performance, and almost no migration occurred in petroleum ether. It is expected to be used in the packaging of organic solvent containers. We also studied the thermal stability of the three types of plasticized PVC. PVC-TH-C had the highest thermal stability. Although the introduction of castor oil reduces the initial decomposition temperature of three types plasticized PVC, when the mass loss was 40%, 50% and 60%, the thermal decomposition activation energy of PVC-TH-C was the highest. This may be related to the existence of triazine ring in THDI. The stable rigid triazine ring structure in THDI effectively improves the overall thermal performance of PVC-TH-C. In the thermal degradation, the three types of internally-plasticized PVC, especially PVC-TH-C, released less harmful gases such as HCl and benzene vapor than pure PVC did. Hence, this strategy contributes to reducing damage to the environment and human health, and this study provides a feasible scheme for efficient utilization of castor oil.

Author contribution

Tianxiang Deng: conceptualization, methodology, writing – Original, Draft, project administration. Shouhai Li: formal analysis, review & editing. Xiaohua Yang: investigation. Haiyang Ding: investigation. Lina Xu: review & editing. Mei Li: funding acquisition, resources, supervision.

Conflicts of interest

The authors declare that there is no conflict of interest.

Acknowledgements

This work was supported by the National Natural Science Foundation of China (grant number: 31971597).

References

1 L.-F. Fang, B.-K. Zhu, L.-P. Zhu, H. Matsuyama and S. Zhao, *J. Membr. Sci.*, 2017, **524**, 235–244, DOI: **10.1016/j.memsci.2016.11.026**.

2 J. M. Beveridge, H. M. Chenot, A. Crich, A. Jacob and M. G. Finn, *Langmuir*, 2018, **34**, 10407–10412, DOI: **10.1021/acs.langmuir.7b03115**.

3 M. Li, J. Jiang, S. Li, K. Huang and J. Xia, *Adv. Mater. Res.*, 2013, **721**, 173–176, DOI: **10.4028/www.scientific.net/AMR.721.173**.

4 F. Chiellini, M. Ferri, A. Morelli, L. Dipaola and G. Latini, *Prog. Polym. Sci.*, 2013, **38**, 1067–1088, DOI: **10.1016/j.progpolymsci.2013.03.001**.

5 A. Earla, L. Li, P. Costanzo and R. Braslau, *Polymer*, 2017, **109**, 1–12, DOI: **10.1016/j.polymer.2016.12.014**.

6 F. Mayer, D. Stalling and J. Johnson, *Nature*, 1972, **238**, 411–413, DOI: **10.1038/238411a0**.

7 A. Earla and R. Braslau, *Macromol. Rapid Commun.*, 2014, **35**, 666–671, DOI: **10.1002/marc.201300865**.

8 K. W. Lee, J. W. Chung and S.-Y. Kwak, *Green Chem.*, 2016, **18**, 999–1009, DOI: **10.1039/C5GC02402A**.

9 P. Jia, M. Zhang, L. Hu, G. Feng, C. Bo and Y. Zhou, *ACS Sustainable Chem. Eng.*, 2015, **3**, 2187–2193, DOI: **10.1021/acssuschemeng.5b00449**.

10 P. Jia, M. Zhang, L. Hu, G. Feng, C. Bo, C. Liu and Y. Zhou, *Ind. Crops Prod.*, 2015, **76**, 590–603, DOI: **10.1016/j.indcrop.2015.07.034**.

11 C. P. McCoy, N. J. Irwin, J. G. Hardy, S. J. Kennedy, L. Donnelly, J. F. Cowley, G. P. Andrews and S. Pentlavalli, *Eur. Polym. J.*, 2017, **97**, 40–48, DOI: **10.1016/j.eurpolymj.2017.09.030**.

12 H. Chu and J. Ma, *Korean J. Chem. Eng.*, 2018, **35**, 2296–2302, DOI: **10.1007/s11814-018-0118-5**.

13 P. Jia, Y. Ma, M. Zhang, L. Hu, Q. Li, X. Yang and Y. Zhou, *Sci. Rep.*, 2019, **9**, 1766, DOI: **10.1038/s41598-018-38407-4**.

14 P. Jia, Y. Ma, Q. Kong, L. Xu, Y. Hu, L. Hu and Y. Zhou, *Mater. Today Chem.*, 2019, **13**, 49–58, DOI: **10.1016/j.mtchem.2019.04.010**.

15 P. Jia, L. Hu, X. Yang, M. Zhang, Q. Shang and Y. Zhou, *RSC Adv.*, 2017, **7**, 30101–30108, DOI: **10.1039/C7RA04386D**.

16 V. Najafi and H. Abdollahi, *Eur. Polym. J.*, 2020, **128**, DOI: **10.1016/j.eurpolymj.2020.109620**.

17 B. Bouchoul, M. T. Benaniba and V. Massardier, *J. Vinyl Addit. Technol.*, 2014, **20**, 260–267, DOI: **10.1002/vnl.21356**.

18 G. Feng, P. Jia, L. Zhang, L. Hu, M. Zhang and Y.-h. Zhou, *Korean J. Chem. Eng.*, 2015, **32**, 1201–1206, DOI: **10.1007/s11814-014-0288-8**.

19 J. Kim, G. Zhang, M. Shi and Z. Suo, *Science*, 2021, **374**, 212–216, DOI: **10.1126/science.abg6320**.

20 N. S. Vrandečić, I. Klarić and T. Kovačić, *J. Therm. Anal. Calorim.*, 2003, **74**, 171–180, DOI: **10.1023/a:1026338121916**.

21 H. Qu, X. Liu, J. Xu, H. Ma, Y. Jiao and J. Xie, *Ind. Eng. Chem. Res.*, 2014, **53**, 8476–8483, DOI: **10.1021/ie404297r**.

22 S. Levchik and E. Weil, *Polym. Adv. Technol.*, 2004, **15**, 691–700, DOI: **10.1002/pat.526**.

23 G. Botelho, A. Queiros, S. Liberal and P. Gijsman, *Polym. Degrad. Stab.*, 2001, **74**, 39–48, DOI: **10.1016/S0141-3910(01)00088-X**.